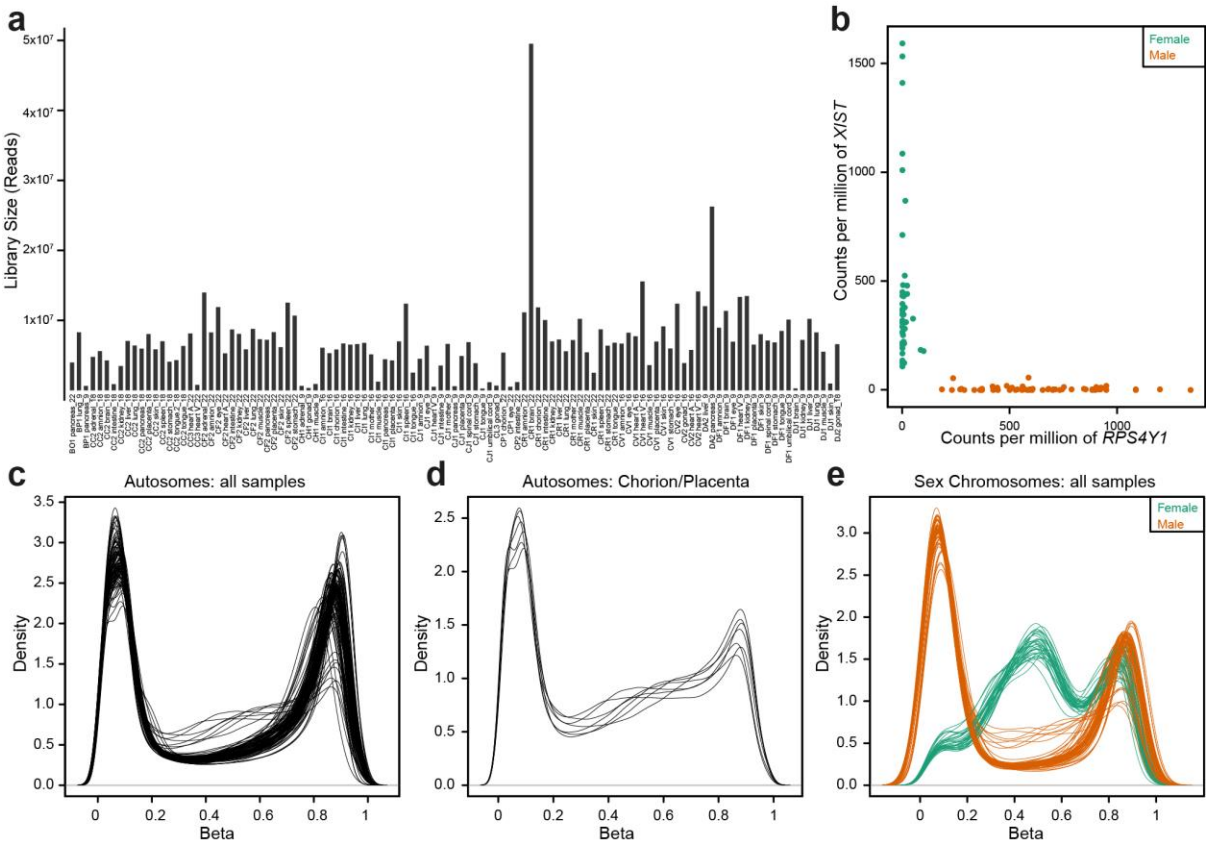

Supplementary Figure 1. Quality control of transcriptome and DNA methylome data. **(a)** Library sizes of the 111 NGS transcriptional profiles. **(b)** Expression levels (counts per million, CPM) of the female gene *XIST* and the male gene *RPS4Y1*. **(c-d)** Density plots of the beta values (450K DNA methylation) of the autosomes of all samples **(c)** and only of the chorion and placenta **(d)**. **(e)** Density plot of the beta values (450K DNA methylation) of the sex chromosomes of all samples separated by sex (male and female).

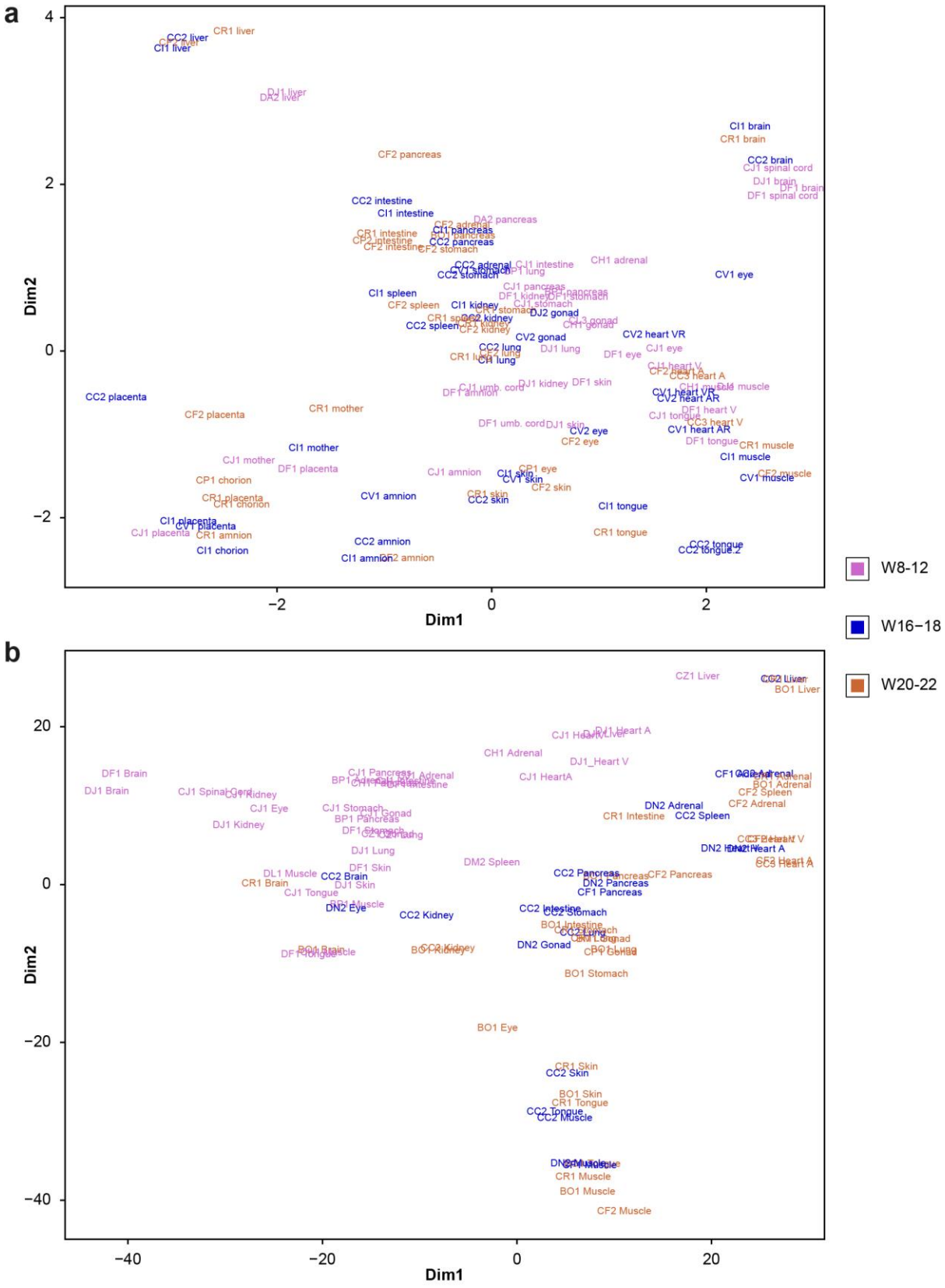
a
b
Dim1
Dim2
W8-12
W16−18
W20-22

Supplementary Figure 2. Multidimensional scaling. (a-b) Multidimensional scaling (Euclidian distance) of the 111 transcriptional profiles (including extraembryonic samples) **(a)** and the 87 DNA methylation profiles of the embryonic samples only (excluding extraembryonic samples) **(b)**. Each sample is named as "embryo ID code_tissue name" and the color code depicts the gestational age group (W8-12 in pink; W16-18 in blue, W20-22 in orange).

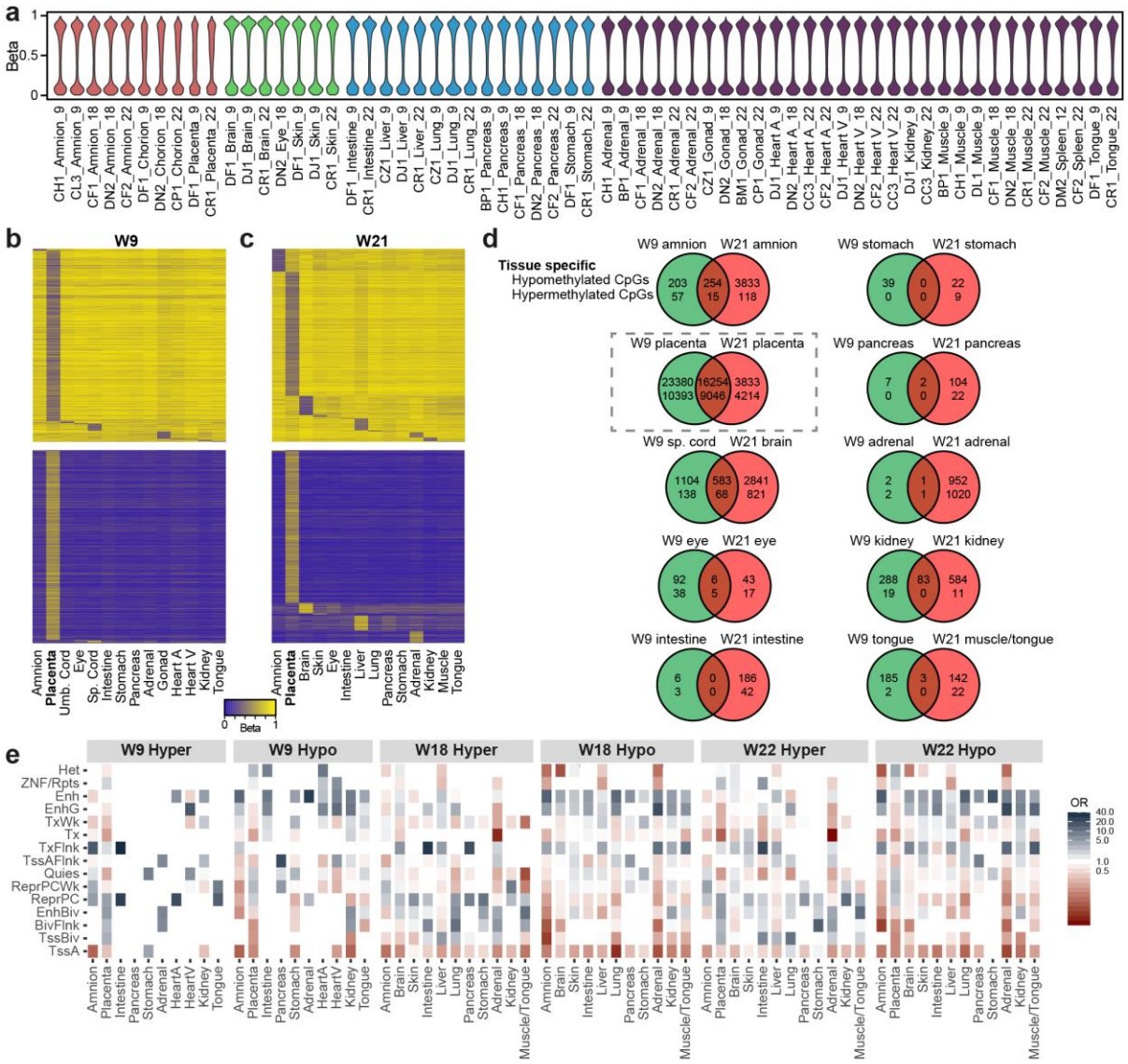

Supplementary Figure 3. DNA methylation signatures during human fetal development. **(a)** Violin plot depicting the distribution of the DNA methylation levels of the remaining samples that were excluded from the three isogenic sets shown in Fig. 3a. **(b-c)** Heatmaps displayed in Fig. 3b,c including the probes of the placenta. **(d)** Venn diagrams showing the overlap between W9 and W21 of tissue-specific hypomethylated CpGs (top) and of hypermethylated (bottom). The dashed-box highlights the large number of tissue specific CpGs in the placenta. **(e)** Enrichment of the identified hyper- and hypomethylated CpGs in the chromatin state segmentations for fetal adrenal, amnion, fetal heart atrium and ventricle, fetal intestine, fetal kidney, adult liver, fetal lung, fetal muscle, adult pancreas, placenta, adult fibroblasts (skin), and fetal stomach given as odds ratio (OR).

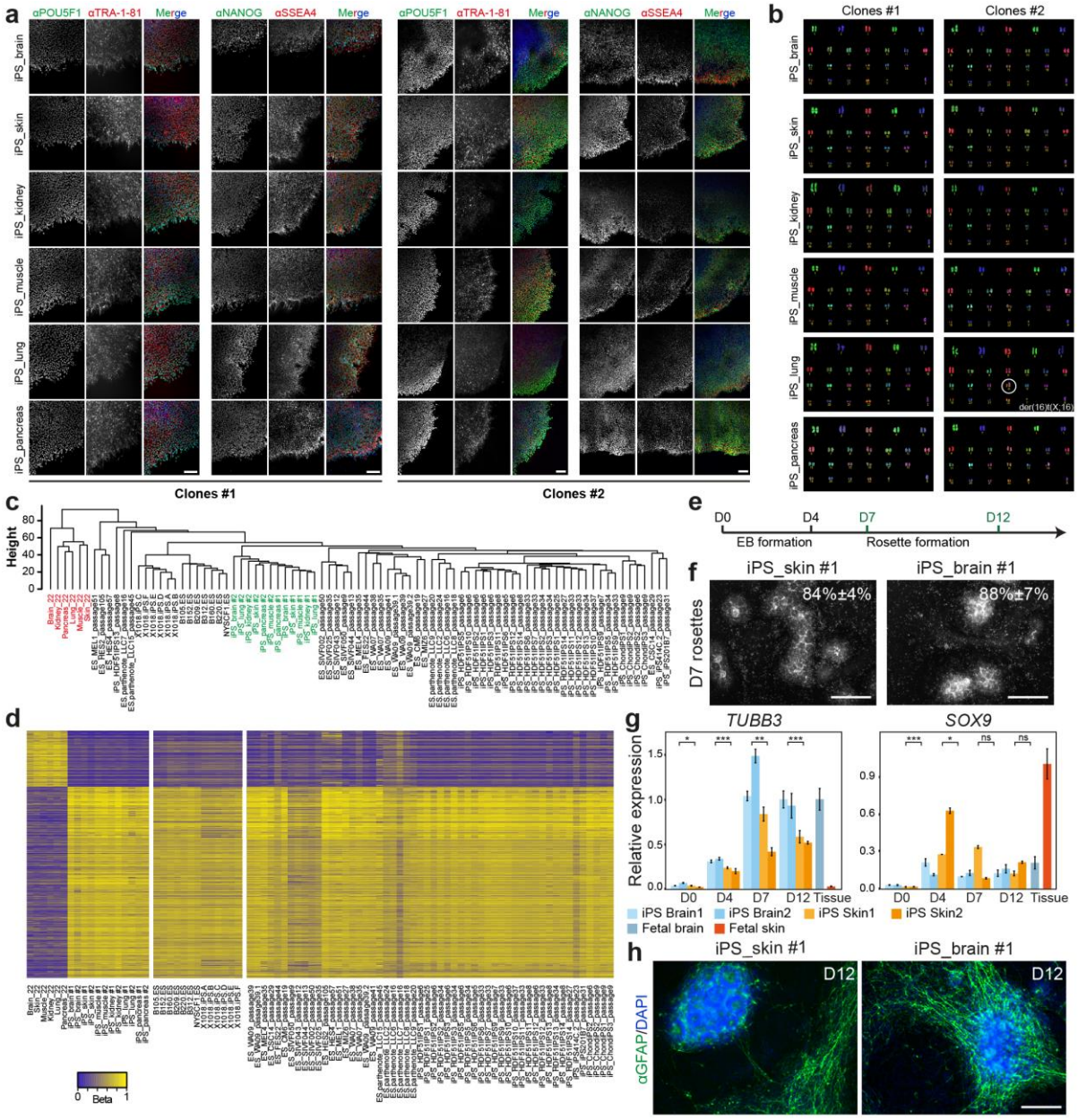

Supplementary Figure 4. Isogenic sets of human iPSCs. (a) Single and merged channels of the immunofluorescence of each of the 12 iPSC clones for POU5F1 and TRA-1-81, and NANOG and SSEA4. Scale bars 100 µm. **(b)** Karyograms of the 12 iPSC clones using COBRA. **(c)** Hierarchical clustering of the 12 iPSC clones (in green) and their tissues of origin (in red) together with two external 450K datasets (Johannesson et al., 2014; Nazor et al., 2012). **(d)** DNA methylation levels of two external datasets regarding the hiPSC-specific hypomethylated (2852 CpGs) and hypermethylated (8772 CpGs) CpG depicted in Fig. 4f. **(e)** Cartoon depicting the neural induction protocol followed and time points of analysis (in

green). **(f)** Dark field picture of embryoid bodies containing rosettes present in culture after 7 days of neural differentiation. Scale bars: 500 µm. **(g)** Relative expression of *TUBB3* and *SOX9* in hiPSCs and fetal brain and skin. Each bar represents mean ± standard deviation of technical triplicates. Significant P values between brain- and skin-hiPSCs at each day are indicated by ns, not significant; * ($p < 0.05$); ** ($p < 0.01$); and *** ($p < 0.001$); Student's t-test (two-tailed). **(h)** Immunofluorescence for the neural marker GFAP after 12 (D12) days of neural differentiation. Scale bars: 200 µm.